Biochimica et Biophysica Acta 1813 (2011) 14–26

Contents lists available at ScienceDirect

Biochimica et Biophysica Acta

journal homepage: www.elsevier.com/locate/bbamcr

Membrane depolarization regulates AMPA receptor subunit expression in cerebellar granule cells in culture

Salvatore Incontro, Jorge Ramírez-Franco, José Sánchez-Prieto, Magdalena Torres *

Departamento de Bioquímica, Facultad de Veterinaria, Universidad Complutense de Madrid, 28040-Madrid, Spain

ARTICLE INFO

Article history:
Received 2 July 2010
Received in revised form 14 October 2010
Accepted 27 October 2010
Available online 4 November 2010

Keywords:
Calcium-dependent homeostatic changes
AMPA receptors
CaMKIV
Cerebellar granule cells

ABSTRACT

The physiological responses of AMPA receptors can be modulated through the differential expression of their subunits and by modifying their number at the cell surface. Here we have studied the expression of AMPA receptor subunits (GluR1–4) mRNAs in cerebellar granule cells grown in depolarizing (25 mM K^+) medium, and we have evaluated the effect of decreasing the [K^+] in the culture medium for 24 h on both GluR1–4 expression (both mRNA and protein) and their presence at the plasma membrane. The expression of the four AMPAR subunits increases as the [K^+] decreases, although the increase in GluR2 and GluR3 was only observed in the cell soma but not in the dendrites. Calcium entry through L-type calcium channel and CaMKIV activation are responsible for the reduction in the expression of AMPA receptor subunits in cells cultured in depolarizing conditions. Indeed, prolonged reduction of extracellular [K^+] or blockage of L-type calcium channels enhanced both the surface insertion of the four AMPAR subunits and the AMPA response measured through intracellular calcium increase. These findings reveal a balanced increase in functional AMPA receptors at the surface of cells that can trigger strong increases in calcium in response to the persistent reduction of calcium entry.

1. Introduction

Physiological responses of AMPA receptors can be modulated by the differential expression of their subunits and by their number at the cell surface. The expression of the four subunits of these receptors is differentially regulated during development [1], and their number in the plasma membrane can be regulated rapidly by controlling their recycling between the plasma membrane and the membranes of intracellular organelles [2–4]. AMPARs are homomeric or heteromeric structures made up from four different subunits, named GluRs 1, 2, 3, and 4 [5,6]. The specific properties of the channels are modified by their subunit composition and, for example, the inclusion of one or more GluR2 subunits in the channel makes it impermeable to Ca^{2+} [7]. This ability of GluR2 to limit AMPAR Ca^{2+} conductance resides in the pore-forming loop, where its structure may be modified by mRNA editing [7]. The expression of AMPARs can be regulated by the cellular environment at both the transcriptional or translational level, for example, by K^+-induced membrane depolarization [8,9]. Moreover, the trafficking of AMPA receptors between the plasma membrane and intracellular compartments can be regulated by the cellular environment or growth conditions [10–12]. Indeed, the variation in the profile of these receptors due to the modification of culture conditions can be considered as a kind of homeostatic plasticity in order to adapt cells to these novel conditions.

In culture, cerebellar granule cells (CGCs) have been used to investigate glutamate receptor-mediated signal transduction and excitotoxicity [13,14]. Differentiating rat granule cells develop survival requirements [15] in vitro that can be met by exposure to high K^+ (> 20 mM) or excitatory amino acids, which mimics the activity-dependent maturation of granule cells by mossy fiber inputs [16,17]. Membrane depolarization enhances calcium entry via voltage-sensitive Ca^{2+} channels (VSCCs), which in turns activates different cascades that involve Ca^{2+}/calmodulin-dependent protein kinases and Ca^{2+}/calmodulin-dependent calcineurin phosphatases [18–20]. This Ca^{2+} signalling should regulate the expression of a large number of proteins, including glutamate ionotropic receptors. The mechanisms regulating the expression of $GABA_A$ and NMDA receptors have been studied extensively in granule cells cultured in different depolarizing conditions [20–22]. However, there are little data regarding

Abbreviations: AMPA, α-amino-3-hydroxyl-5-methyl-4-isoxazole-propionate; AMPAR, AMPA receptor; CHAPS, 3-[(3-cholamidopropyl)dimethylammonio]-1-propanesulfonate; CaMKIV, Ca^{2+}/calmodulin-dependent protein kinase type IV; CGC, cerebellar granule cell; DAPI, 4′,6-diamino-phenylindole dihydrochloride; DIV, days in vitro; FIC, freshly isolated cells; GFAP, green fibrillary acidic protein; IRD, near-infrared fluorescent dye; KA, kainate; NBQX, 2,3-dihydroxy-6-nitro-7-sulfamoyl-benzo(F) quinoxaline; MK-801, (+)-5-methyl-10,11-dihydro-5H-dibenzo[a,b]cyclohepten-5,10-imine hydrogen maleate; NMDAR, NMDA receptor; ROI, region of interest; TBE buffer, Tris borate EDTA buffer; TES, *N*-Tris (hydroxymethyl)methyl-2-aminoethanesulfonic acid; VSCCs, voltage-sensitive calcium channels

* Corresponding author. Tel.: +34 913943891; fax: +34 913943909.
E-mail address: mitorres@vet.ucm.es (M. Torres).

0167-4889/$ – see front matter © 2010 Elsevier B.V. All rights reserved.
doi:10.1016/j.bbamcr.2010.10.016

the expression of AMPAR and their regulation by depolarizing conditions. Furthermore, a simultaneous analysis of the four AMPAR subunits has yet to be performed. In this study, we have examined the expression of the four AMPAR subunits and how the extracellular [K^+] affects their expression (at the mRNA and protein level), their presence at plasma membrane, and their activity in terms of the AMPA-elicited increase in intracellular calcium. Moreover, we have analyzed the involvement of calcium signalling in controlling the expression of these proteins.

2. Materials and methods

2.1. Primary culture of cerebellar neurons

All procedures relating to the care of animals were carried out in accordance with our institute's ethical guidelines for animal experiments and the regulations established in the European Council Directive (86/609/EEC). Primary cultures of dissociated cerebellar neurons were established from the cerebellum of 7-day-old (P7) male or female Wistar albino rat pups according to the protocol described previously [23]. Cerebellar neurons were diluted in Neurobasal A supplemented with B27 (Invitrogen), 20 mM KCl, 0.5 mM glutamine, and a stabilized antibiotic antimycotic solution (Sigma-Aldrich). The cells were seeded onto poly-L-lysine coated coverslips, or in 96- or 6-well tissue culture plates, at a density of $1–3\times10^5$ cell/coverslip, 2×10^5 or 3.5×10^6 cells/well, respectively. The cultures were maintained in a humidified incubator in 5% CO_2 at 37 °C, and after 24 h in culture, 10 μM cytosine-β-D-arabinofuranoside (Sigma-Aldrich) was added to restrict glial cell growth. The cultures were used for experiments at 7 DIV or 14 DIV (days in vitro).

2.2. Cell treatments

To test the effect of neuronal activity, we incubated the 6 DIV cultured neurons for 24 h in medium containing 15 mM KCl. To test the effect of calcium channel blockers, specific inhibitors were added 24 h before carrying out the experiment.

2.3. Immunocytochemistry

Cerebellar granule cells were plated on polylysine-coated coverslips at a density of 100,000 cells/coverslip. The attached cells were rinsed twice with PBS, fixed with 4% formaldehyde in PBS for 15 min at room temperature, briefly rinsed twice with TBS, and then permeabilized for 6 min with 0.2% Triton X-100 in TBS. The cells were then blocked with TBS containing 0.05% Triton X-100 and 10% normal donkey serum for 1 h at 37 °C, and they were then incubated for 24 h at 4 °C with the primary antibodies diluted in TBS containing 5% normal donkey serum and 0.05% Triton X-100: 1:200 rabbit anti-glutamate receptor 1 (GluR1), clone C3T subunit (04-855 Millipore); 1:200 mouse anti-glutamate receptor 2 (GluR2), clone 6 C4 (MAB397 Chemicon [Millipore]); 1:200 mouse monoclonal against glutamate receptor 3 (GluR3) (MAB5416 Chemicon [Millipore]); 1:200 affinity purified anti-rabbit glutamate receptor 4 (GluR4) subunit (06-308 Upstate [Millipore]); 1:500 rabbit anti-Na^+/K^+ ATPase β-1 (Millipore); 1:1000 rabbit anti-MAP2 (Synaptic systems); 1:1000 mouse anti-MAP2 Alexa Fluor 488-conjugated (Chemicon); 1:500 guinea pig polyclonal anti-Bassoon (126 111 Synaptic systems); 1:200 rabbit anti-p-CaMKIV (Thr 196). After washing the coverslips, the cells were incubated with the appropriate fluorescent secondary antibodies diluted in TBS containing 5% normal donkey serum and 0.05% Triton X-100: 1:500 Cy3-conjugated Affinipure Donkey anti-rabbit (Jackson) or 1:500 Cy2-conjugated Affinipure anti-mouse (Jackson). For the double staining immunocytochemistry experiments with GluR and Bassoon, goat anti-rabbit Alexa fluor 488 and goat anti-guinea pig 546 were used as secondary antibodies, respectively, using normal goat serum in the blocking step (10%) and in the incubation with primary antibody (5%). Following several washes in PBS, the coverslips were mounted with prolong antifade (Invitrogen), and the cells were viewed with a Nikon Diaphot microscope equipped with a 40× 1.3 (NA) or 100× 1.3 (NA) oil immersion fluor objective, a mercury lamp light source, and fluorescein or rhodamine Nikon filter sets. Images were obtained using a slow-scan CCD camera (Hamamatsu C4880) operating at 12-bit digitalization (4096 levels) and the camera output was stored using a computerized imaging system (Kinetic Imaging, Ltd.).

For control staining to confirm the specificity of the antibodies used, the cells were incubated with the secondary antibodies alone in the absence of primary antibodies, and for p-CaMKIV immunocytochemistry, the cells were pre-incubated with a control peptide antigen.

For the quantitative analysis, all the images were acquired with identical settings of brightness and contrast. The ROIs (regions of interest) were selected with Igor Pro software and spurious ROIs were removed manually [24]. Staining intensities were measured as greyscale values (ranging from 0 to 255) using the Image J v1.39f (http://rsb.info.nih.gov/ij). The integrated value was calculated by summing the grey values of each pixel, and the mean intensity value was calculated by dividing the integrated intensity by the number of pixels. Background subtraction was performed by applying a medial filter (3×3 pixel radius) [25] to remove noise and to approximate the distribution of staining intensity to a median value. The values were normalized to MAP-2 labelling (internal control for quantitative analysis) and used to compare signal intensities between control and treated cells. For p-CaMKIV immunocytochemistry, image analysis was only performed on cells marked with 4′,6-diamino-2-phenylindole dihydrochloride (DAPI, Molecular Probes, Eugene, OR, USA) in each field and binary image masks were created after background subtraction of p-CaMKIV and DAPI positive staining to define the region of interest (ROI) for analysis. Automatic thresholding with the Isodata algorithm [26] was then used to convert the image into a binary mask that included all the fluorescence emissions above background. The DAPI staining mask was used to define the nuclear ROI. Using the image calculator, the DAPI mask was subtracted from the p-CaMKIV mask to create a staining mask defining the cytoplasmic ROI. All of these ROI masks were then applied to the original p-CaMKIV staining images to separate nuclear and cytoplasmic staining within each field. Quantitative fluorescence data were exported from Image J to Origin Pro 8 software for further analysis and presentation. Therefore, nuclear and cytoplasmic staining intensities were compared to give the nuclear/cytoplasmic ratio as a relative measure of p-CaMKIV nuclear localization.

2.4. Preparation of protein extracts

Cells were homogenized in Tris–HCl 25 mM [pH 7.6], containing 150 mM NaCl, 5 mM EDTA, and protease inhibitors (Pierce), and then centrifuged for 10 min at 800×*g*. The supernatant recovered was centrifuged at 30,000×*g* for 40 min to obtain a membrane-enriched fraction (pellet), and the resulting pellet was resuspended in buffer containing 10 mM Tris–HCl [pH 7.4], 2 mM EDTA, 10 mM CHAPS, and protease inhibitors.

2.5. Western blotting

Equal amounts of total protein for each sample were separated on 8–10% sodium dodecyl sulphate-polyacrylamide gels and electrophoretically transferred to nitrocellulose membranes (GE Healthcare) as described previously [27]. The membranes were probed with the appropriate primary antibodies: 1:1000 anti-rabbit glutamate receptor 1 (GluR1) subunit (Upstate); 1:1000 anti-rabbit glutamate receptor 4 (GluR4) subunit (Upstate); 1:1000 rabbit anti-Na^+/K^+ ATPase β-1 (Millipore). After several washes, the membranes were incubated with the corresponding IRD-labelled secondary antibody

diluted 1:15,000 (LiCor biosciences) and the blots were scanned in an Odissey Infrared imaging system comparing the immunoreactive proteins by measuring the fluorescent intensity by densitometry. The ATPase β-1 signal was used to normalize for loading differences, and the Odissey 2.0 software was used for quantification.

2.6. Viability

Cell viability was determined by measuring cellular lactate dehydrogenase (LDH) release using a commercial fluorimetric kit (CytoTox-ONE™, Promega). The measurements were expressed as the percentage of the total signal measured in several wells where the cells were previously incubated with methanol.

2.7. RT-PCR and real-time RT-PCR reactions

Total RNA was extracted from cells using the RNeasy kit (Quiagen), it was quantified using the RiboGreen™ RNA Quantification Kit (Invitrogen) [28], and RT-PCR reactions were performed in two steps as described previously [23]. The first-strand cDNA was synthesized with MultiScribe™ reverse transcriptase (Applied Biosystems) in RT buffer containing 5.5 mM $MgCl_2$, 500 μM of each dNTP, 2.5 μM random hexamers, 0.4 U/ml RNAse inhibitor, and 3.125 U/ml MultiScribe™ reverse transcriptase. The reactions were performed in a final volume of 50 μl containing 1 μg of RNA and primer-RNA template binding was maximized through a 10-min incubation at 25 °C. Reverse transcription was carried out at 48 °C for 30 min, and the reverse transcriptase was inactivated before performing the PCR reactions by heating the samples at 95 °C for 5 min. The specific PCR oligonucleotides for the four AMPA subunits were designed on the basis of the published sequence and they are summarized in Table 1. RT-PCR was carried out in a Mastercycler personal Eppendorf and the PCR products were resolved in a 2% agarose gel in TBE containing 0.1 μl/ml of SYBR® safe DNA gel stain (Molecular Probes) at 100 V.

For quantitative RT-PCR, we used the predesigned primer and MGB probes from Applied Biosystems for GluR1 (Rn00709588, lot 493728), GluR2 (Rn00568514, lot 483600), GluR3 (Rn00583547, lot 399310), and GluR4 (Rn0056844, lot 353366). Kits with MGB probes to amplify GAPDH or 18S rRNA from rat were used as endogenous controls (Applied Biosystems). PCR reactions were followed in a 9800 Fast Thermal Cycler (Applied Biosystems) with TaqMan Gold PCR reagents. In order to calculate the efficiency (η) of each reaction, standard plots were constructed with different cDNA concentrations and the efficiency was calculated as ($\eta = [10^{-(1/\text{slope})}] - 1$).

2.8. GluR2 mRNA edition assay

To define the status of the GluR2 subunit in terms of mRNA editing, RT-PCR was carried out using the following primers to amplify a 351-bp region of the mRNA containing the Q/R edition site: GluR2 accession number NM_017261: forward, base position 2003, 5′ ATCAAGAAG CCTCAGAAGTCCAAA3′; reverse, base position 2353, 5′ TAAGTTAGCCGTGTA GGAGGAGATTAT3′. After RT-PCR amplification of the total RNA (94 °C, 10 min to activate polymerase and 40 cycles, 95 °C 15 s, 62 °C, 1 min; followed by holding at 72 °C, 7 min), the PCR product was purified with QIAquick PCR purification kit (Quiagen) according to the manufacturer's instructions. An aliquot of the sample was digested with *Bbv*I to evaluate the ratio of the unedited/edited forms given that the A to G conversion in the edited sequence of the GluR2 mRNA abolishes the *Bbv*I restriction enzyme site present in the unedited form. Hence, we measured the changes in the unedited/edited through the loss of sensitivity to the *Bbv*I digestion, using the pBR322 plasmid as a positive control for *Bbv*I activity. Another aliquot of the PCR product was enzymatically digested with AciI, which specifically digests the edited form to generate two DNA fragments of 250 and 100 bp. The DNA fragments were resolved in a 2% agarose gel in TBE containing 0.1 μl/ml of SYBR® safe DNA gel stain (Molecular Probes) at 100 V.

2.9. CaMKIV silencing assay

A siRNA designed to selectively silence CaMKIV (Dharmacon, Thermo Scientific, CO) was added to cells after 4 DIV in medium supplemented with B27 (Invitrogen), 20 mM KCl, 0.5 mM glutamine and the stabilized antibiotic antimycotic solution (Sigma-Aldrich). Total RNA was extracted after 72 h, and the amount of the AMPAR subunit mRNAs determined as indicated above. CaMKIV silencing was confirmed by immunocytochemistry.

2.10. Measurement of $[Ca^{2+}]_i$ in cerebellar granule cells

2.10.1. Cell populations

Increases in $[Ca^{2+}]_i$ were determined using a FLUOstar OMEGA fluorescence microplate reader equipped with two injectors (BMG LabTechnologies, Offenburg, Germany), as described elsewhere [29]. Granular neurons maintained in culture for 7 DIV were loaded with 5 μM Fluo-4 acetoxy methylester (Fluo-4 AM) in TES buffer (composition in mM: NaCl 140, KCl 5, $CaCl_2$ 1.33, $MgCl_2$ 1, glucose 10 and TES 10 [pH 7.4]) for 45 min at 37 °C, and they were subsequently washed twice with fresh buffer before further incubating for 15 min. All experiments were performed at 37 °C, and the data were collected at 0.5 or 1-s intervals. Fluorescence was excited using a 485 nm filter and read through a 520-nm long-pass emission filter. To measure the Ca^{2+} responses in cells, basal fluorescence was first monitored for 4 s before the cells were stimulated with 50 μM AMPA (final concentration) plus cyclothiazide 10 μM, the fluorescence was monitored for a further 10 s and the cells were then stimulated with 30 mM KCl. The results are expressed as F/F_0, with F being the fluorescence at each time and F_0 the initial fluorescence.

2.10.2. Individual cells

The calcium responses in individual cells were measured according to the method described previously [30]. Cerebellar granule cells were plated on polylysine-coated coverslips at a density of 200,000 cells/coverslip, and they were maintained in culture for 7 DIV. The cells were loaded with 3 μM Flura-2 acetoxy methylester (Fura-2 AM) for 50 min at 37 °C in HBM buffer (composition in mM: NaCl 140, KCl 5, $CaCl_2$ 1.33, $MgSO_4$ 1.2, NaH_2PO_4 1.2, $NaHCO_3$ 5, glucose 10, and HEPES 10 [pH 7.4]), and then washed twice with fresh HBM before further incubating for 15 min to allow deacetylation of FURA-2. A perfusion chamber was

Table 1
Oligonucleotides used for conventional PCR experiments.

	Accession number	Forward primer: base position and sequence	Reverse primer: base position and sequence	Amplified fragment (bp)
GluR1	NM_031608	2612, 5′ TGTGGCAGGCGTGTTCTACA3′	2762, 5′ CCGTATGGCTTCATTGATGGA3′	151
GluR2	NM_017261	2003, 5′ATCAAGAAGCCTCAGAAGTCCAAA3′	2103, 5′CTGACCCCAATGTAGGCAAAC3′	101
GluR3	NM_032990	1800, 5′GAAGAACCTCGTGACCCACAA3′	1950, 5′ACCAAACCCCTCCAACAATG3′	151
GluR4	NM_017263	1775, 5′CTTCTTGGACCCTCTGGCCTAT3′	1925, 5′CTGGTCACTGGGTCCTTCCTT3′	151

carved in a small Petri dish that was then mounted on a Nikon inverted stage microscope. Medium was fed into the chamber by gravity at 1–1.5 ml/min from a prewarmed (37 °C) reservoir, and it was continuously removed by aspiration. Cells were illuminated alternately at 350 and 380 nm for 0.8 s through a 40× 1.3 N.A oil immersion fluor objective with the aid of a monochromator (Kinetic Imaging, Ltd.), and the fluorescence emitted by the cells was collected through a band-pass filter centered at 510 nm. The video images were obtained using a slow-scan CCD camera (Hamamatsu C4880) operating at 12-bit digitalization (4096 levels), and the output from the camera was stored on a computerized imaging system (Kinetic Imaging, Ltd.). Background images (without fura-2 fluorescence) at F350 and F380 were acquired and subtracted from each series of F350 and F380 images. Thus, the F350/380 image ratios were obtained using Kinetic Imaging software and the ratio images were stored as 32-bit floating point number data, avoiding clipping by binary digitalization. Cells were clearly identified by their morphology, and they were stimulated through 10-s pulses of the indicated stimulus (indicated in each graph by a bar), in the presence or absence of different drugs applied to the cells by switching the perfusion solution.

2.11. Immunohistochemistry

Cerebellar preparations obtained from 14-day-old or adult rats were processed for immunofluorescence studies as follows. Animals were anesthetized with ketamine/xylazine and perfused first with saline serum for 5 min and then with 4% paraformaldehyde in 0.1 M PBS [pH 7.0] for 10 min. The entire brain was then removed and fixed overnight in the same solution and then cryoprotected in 30% (wt/vol) sucrose in 0.1 M PB at 4 °C before embedding the brain in Tissue-Tek® OCT

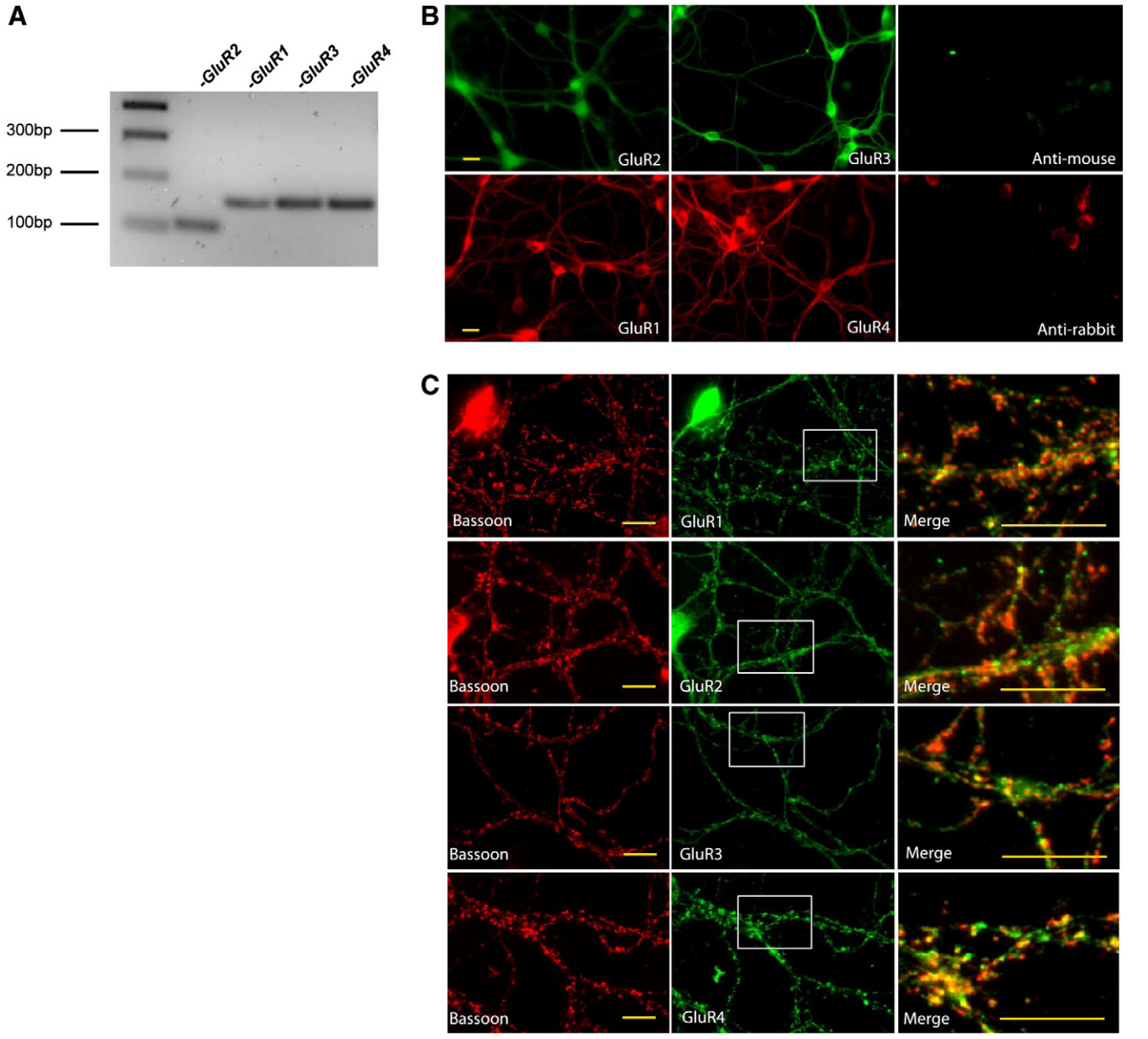

Fig. 1. Cerebellar granule neurons express the four AMPA receptor subunits: mRNA and protein. (A) RT-PCR analysis of AMPAR subunit expression in cells maintained for 7 days in culture (7 DIV). Lane 1: 100-bp molecular size markers, lane 2: GluR2, lane 3: GluR1, lane 4: GluR3, lane 5: GluR4. (B) Specific labelling of granule cells (soma and neurites) with mouse anti-GluR2, rabbit anti-GluR1, mouse anti-GluR3, rabbit anti-GluR4, control for the anti-mouse secondary antibody, and control for the anti-rabbit secondary antibody. Scale bars: 10 μm (images taken with a 40× objective). (C) Co-localization of AMPAR subunits (middle panels) with the presynaptic marker bassoon (left panels) and amplified merged images (right panels) of the boxed areas (images taken with a 100× objective). Scale bars: 10 μM.

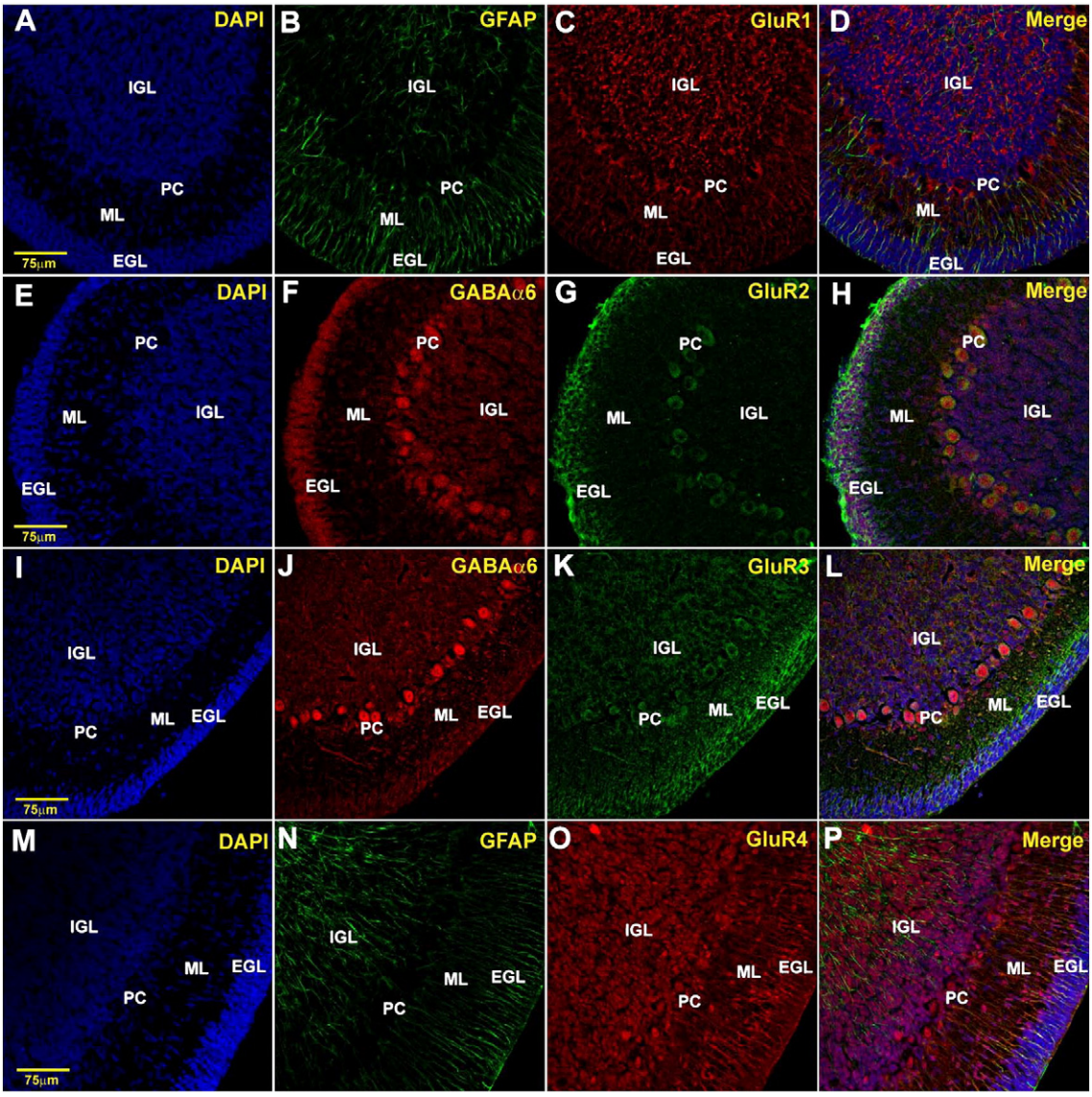

Fig. 2. Confocal immunohistochemistry for AMPAR subunits expressed in the cerebellum of 14-day-old rats (P14). Sections of the cerebellum labelled with DAPI (panels A, E, I, and M) and immunostained with an antibody against $GABA_A$ α_6 (panels F and J). Cerebellum sections immunostained with an antibody against GluR1 (panel C), GluR2 (panel G), GluR3 (panel K), or GluR4 (panel O). Triple merged images of DAPI, GFAP, and GluR1 (panel D). Triple merged images of DAPI, $GABA_A$ α6, and GluR2 (panel H). Merged images of DAPI, $GABA_A$ α6, and GluR3 (panel L) or of DAPI, GAFP, and GluR4 (panel P). Scale bar: 75 μm. EGL: external granular layer, IGL: internal granular layer, ML: molecular layer, and PC: Purkinje cell layer.

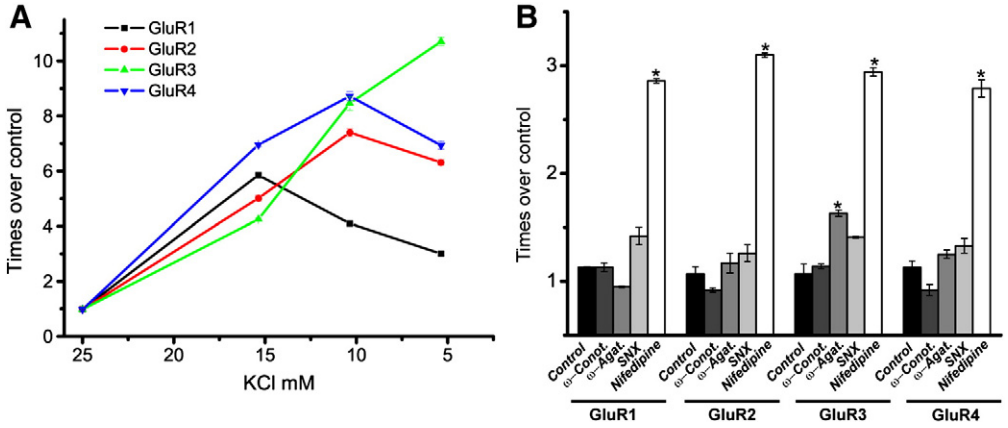

Fig. 3. AMPAR subunit mRNA expression varies with the KCl concentration in the culture medium. (A) Effect on the expression of these mRNAs of maintaining the cells for the last 24-h in culture at different $[K^+]$ at 7 DIV. Cells were cultured in control conditions (25 mM K^+) for 6 days and then switched to culture media containing the $[K^+]$ indicated for 24 h. (B) Effect of a 24-h exposure to different calcium channels blockers on the amount of mRNAs in 7 DIV cells. Values are expressed as the fold increase over the control values for each mRNA. Results are expressed as the mean ± SE of twelve determinations performed with at least four different cultures ($n = 12$, $^*p < 0.01$, t-test).

compound. Cryostat sections (30 μm: CM1850 UV, Leica Microsystems, Barcelona, Spain) of the cerebellum were obtained by latero-medial sectioning of the brain, and consecutive serial sections were collected from each brain in petri dishes containing 1–2 ml 0.1 M phosphate buffer (PB) to obtain a complete series for the various antibodies used. Cerebellar sections were then selected manually, washed with PBS (several times, 5 min each), and non-specific binding was blocked by incubating them for 60 min with 5% normal goat antiserum (Jackson Laboratories) containing 0.3% Triton X-100. The sections were incubated with the primary antibodies diluted in 1% normal goat serum and 0.3% Triton X-100 for 24 h at 4 °C in a humidified chamber. The primary antibodies used were raised against: GluR1 (affinity purified rabbit

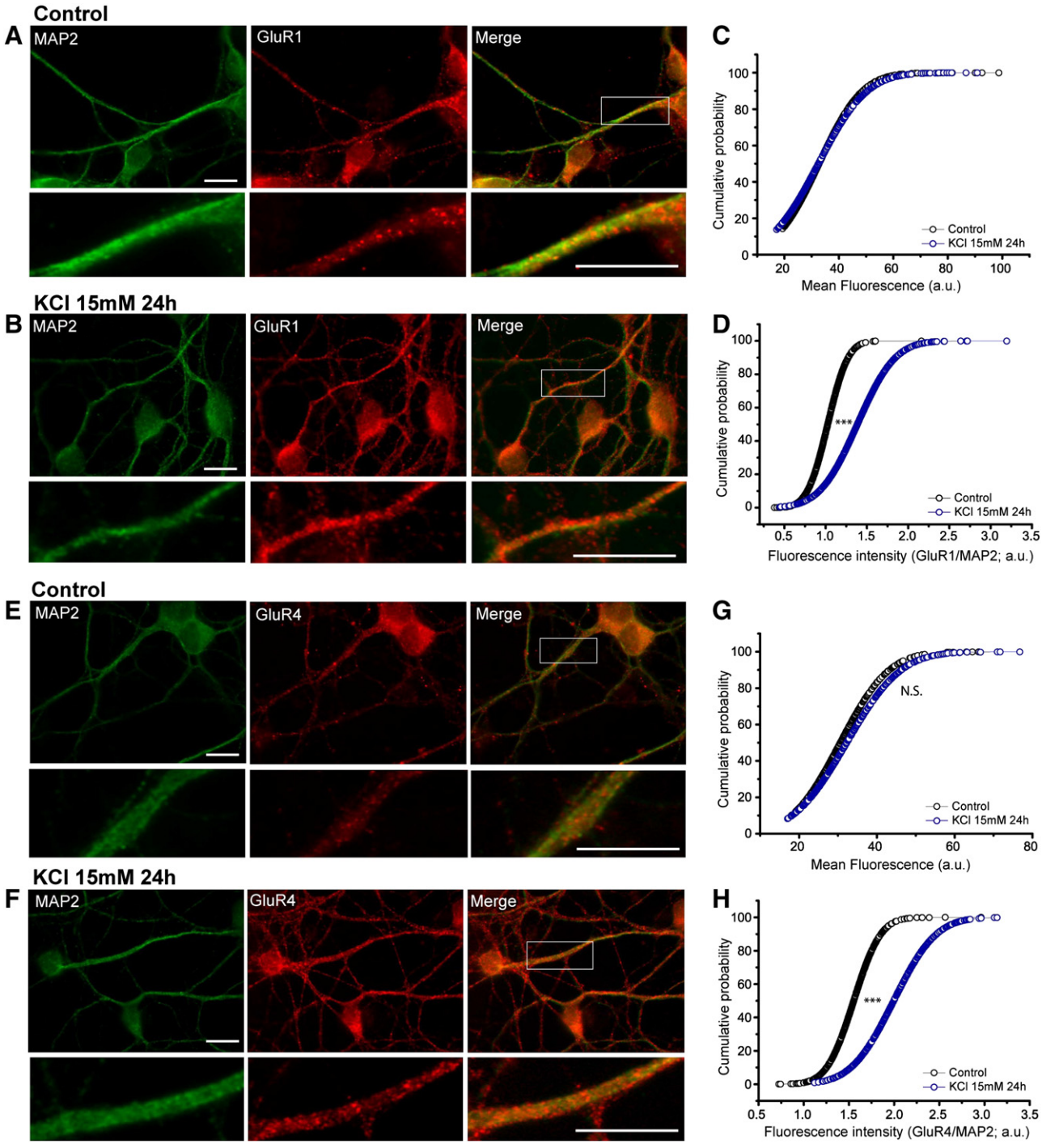

Fig. 4. GluR1, GluR4, and MAP-2 immunodetection in 7 DIV cells maintained in control (25 mM K^+) conditions (A and E) or for the last 24 h in a medium containing 15 mM K^+ (B and F). MAP-2: immunocytochemistry with mouse anti-MAP-2. GluR1: immunocytochemistry with rabbit anti-GluR1. GluR4: immunocytochemistry with rabbit anti-GluR4. (C) Cumulative probability plots of the mean MAP-2 fluorescence intensity of cells also labelled with anti-GluR1 (MAP-2 mean intensity: 30.76 ± 1.53 and 32.21 ± 1.75 a.u. for control (770 ROIs) or low KCl (623 ROIs), respectively, $p > 0.05$, Mann–Whitney test and Kolmogorov–Smirnov test). (D) Cumulative probability plots for the ratio mean GluR1/MAP-2 fluorescence intensity (***$p < 0.001$, Mann–Whitney test and Kolmogorov–Smirnov test). GluR1 mean intensity: 30.92 ± 0.27 and 39.53 ± 0.49 a.u. for control and low K^+, respectively. (G) Cumulative probability plots of the mean MAP-2 fluorescence intensity of cells also labelled with anti-GluR4 (MAP-2 mean intensity: 29.32 ± 1.44 and 31.72 ± 0.71 a.u. for control (1228 ROIs) and low KCl (532 ROIs), respectively. $p > 0.05$, Mann–Whitney test and Kolmogorov–Smirnov test). (H) Cumulative probability plots for the ratio mean GluR4/MAP-2 fluorescence intensity (***$p < 0.001$, Mann–Whitney test and Kolmogorov–Smirnov test). GluR4 mean intensity: 29.68 ± 2.07 and 45.21 ± 2.05 a.u. for control and low K^+, respectively. Scale bars: 10 μm. Merge: merged image of immunostaining with both antibodies, insert 3× magnification of the boxed regions.

antiserum, 1:200, Millipore), GluR4 (affinity purified rabbit antiserum, 1:200, Millipore), GluR2 (a mouse monoclonal, clone 6-C-4, 1:300, Millipore), GluR3 (a mouse monoclonal, clone 3-B-3, 1:200, Millipore), glial fibrillary acidic protein (a mouse monoclonal, clone G-A-5, 1:400, SIGMA), and $GABA_A$ receptor α_6 subunit (affinity purified rabbit polycolonal antiserum, 1:500, Millipore). After washing, the sections were incubated for 2 h in the dark at room temperature with the secondary antibodies appropriately matched to the species in which the primary antibody was raised: goat anti-mouse Alexa fluor 488 and goat anti-rabbit Alexa fluor 594 (both diluted at 1:200; Molecular Probes,

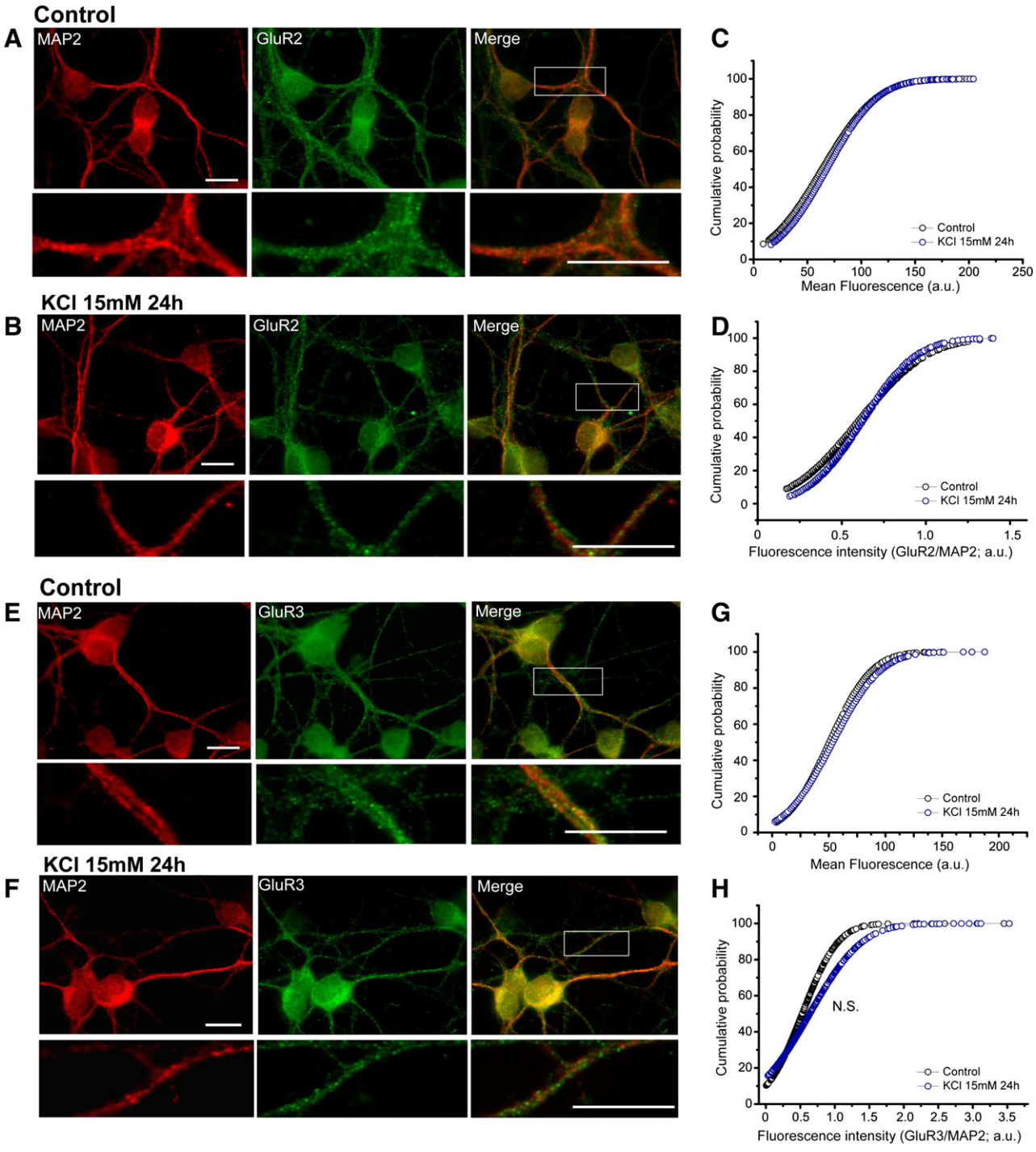

Fig. 5. GluR2, GluR3, and MAP-2 immunodetection in 7 DIV cells maintained in control (25 mM K^+) conditions (A and E) or for the last 24 h in a medium containing 15 mM K^+ (B and F). MAP-2: immunocytochemistry with rabbit anti-MAP-2 in permeabilized cells. GluR2: immunocytochemistry with mouse anti-GluR2 in permeabilized cells. GluR3: immunocytochemistry with mouse anti-GluR3 in permeabilized cells. (C) Cumulative probability plots of mean MAP-2 fluorescence intensity of the cells also labelled with anti-GluR2 (MAP-2 mean intensity: 66.8 ± 3.8 and 66.9 ± 6.1 a.u. for control (924 ROIs) or low K^+ (897 ROIs), respectively, $p > 0.05$, Mann–Whitney test and Kolmogorov–Smirnov test). (D) Cumulative probability plots for the ratio mean GluR2/MAP-2 fluorescence intensity ($p > 0.05$, Mann–Whitney test and Kolmogorov–Smirnov test). GluR2 mean intensity: 32.1 ± 1.4 and 33.6 ± 1.84 a.u. for control and low K^+, respectively. (G) Cumulative probability plots of the mean MAP-2 fluorescence intensity of cells also labelled with anti-GluR3 (mean MAP-2 intensity: 40.25 ± 0.81 and 41.69 ± 1.14 a.u. for control (374 ROIs) or low K^+ (607 ROIs), respectively, $p > 0.05$, Mann–Whitney test and Kolmogorov–Smirnov test). (H) Cumulative probability plots for the ratio mean GluR3/MAP-2 fluorescence intensity ($p > 0.05$, Mann–Whitney test and Kolmogorov–Smirnov test). Mean GluR3 fluorescence intensity 18.60 ± 1.98 and 18.47 ± 1.06 a.u. for control and low K^+, respectively. Scale bars = 10 μm. Merge: merged image of both immunostaining images, insert 3× magnification of the boxed area.

Eugene, OR, USA). After washing with PBS (several times, 10 min each), the sections were mounted onto poly-lysine-coated slides with Prolong Gold® antifade reagent containing 4′,6-diamino-2-phenylindole dihydrochloride (DAPI, Molecular Probes, Eugene, OR, USA). The labelled sections were examined under an Axioplan 2 fluorescence microscope (Carl Zeiss Microimaging GmbH, Göttingen, Germany) equipped with the appropriate filter sets, they were photographed with a Spot-2 digital camera (Diagnostic Instruments, Sterling Heights, MI, USA), and the images were stored digitally as 12-bit images using Leica confocal software.

3. Results

3.1. Cerebellar granule cells express the four subunits of the AMPA receptors in function of the K^+ concentration in the culture medium

Rat cerebellar granule cells maintained for 7 days in vitro (DIV) express mRNA (Fig. 1A) and protein (Fig. 1B and C) for each of the four AMPA receptor subunits. These proteins co-localize well with the presynaptic marker bassoon, indicating that they are localized to the synapse (Fig. 1C). To analyze whether these proteins are expressed at equivalent development stages in vivo, immunohistochemistry was performed on cerebellum sections from 14-day-old and adult rats (Fig. 2 and Supplementary material Fig. S1). In sections from 14-day-old rats, DAPI-labelled cells could be seen in the internal granular layer (IGL), the Purkinje cell layer (PC) that could not yet be distinguished from the IGL, the external granular layer (EGL) that was still evident at these stages, and the cells migrating through the molecular layer (ML: Fig. 2A, E, I, and M). GFAP immunoreactivity (ir) was evident in Bergmann glial cell bodies (BG) in the PC and the IGL, as well as in the Bergmann glial fibers (BF) arranged in parallel and directed toward the outer surface of the molecular layer (Fig. 2B and N). Strong GluR1-ir (Fig. 2C) and GluR4-ir (Fig. 2O) were observed in the internal granular layer (IGL), which is specifically labelled with anti-$GABA_A$ α_6 (Fig. 2F and J), a marker of the terminal differentiation of granule cells [31]. Very weak GluR2-ir was observed in the IGL (Fig. 2G), whereas GluR2 specifically labelled the Purkinje (PC) cell layer and the external granular layer (EGL), which was also labelled with anti-$GABA_A$ α_6. Weak and diffuse GluR3-ir was evident in the IGL, PC, and EGL, and although the staining was not intense, it was a little stronger in the EGL (Fig. 2K).

Since it is well known that the membrane potential regulates the expression of different genes in granule neurons, tonic depolarization was maintained by culturing the cells in the presence of 25 mM K^+. We wondered whether the expression of AMPAR mRNA transcripts was affected by these depolarizing conditions. To assess this, cells were cultured in standard conditions for 6 days and then switched to

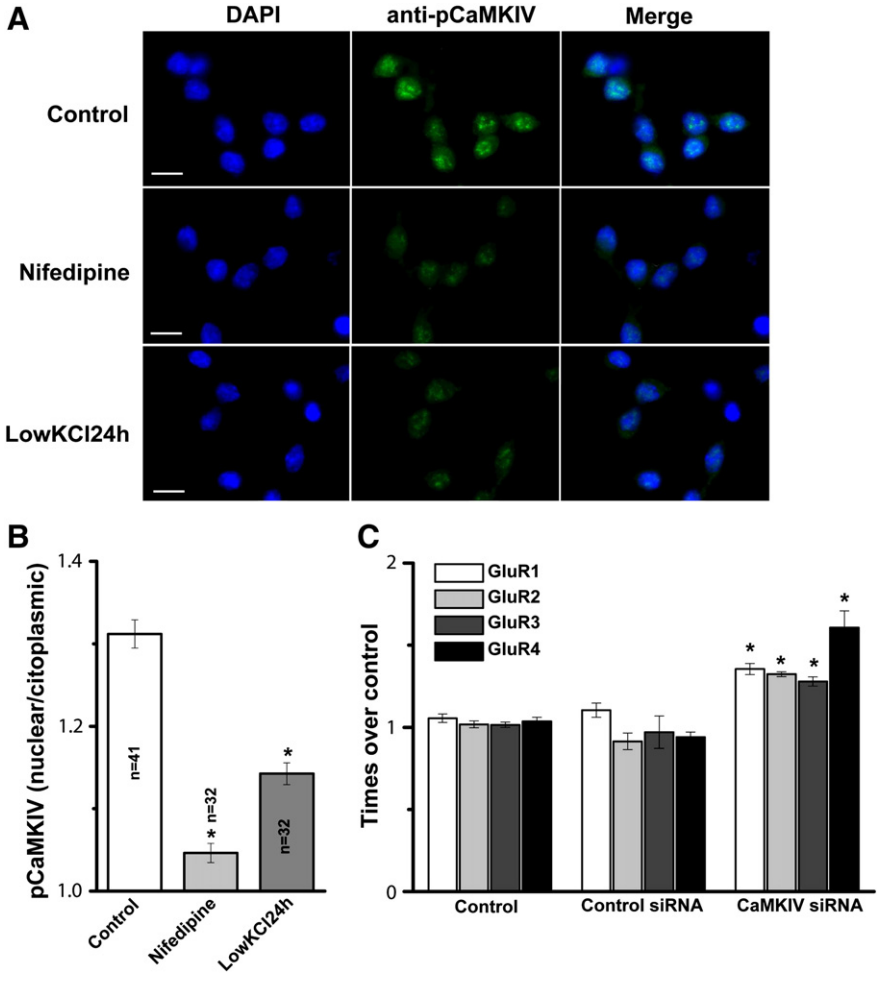

Fig. 6. Phospho-CaMIV immunodetection in cells 7 DIV maintained in control (25 mM K^+) conditions or subjected to different treatments for 24 h (15 mM K^+ or 5 μM nifedipine). DAPI labelling (left panels), pCaMIV (middle panels), and merged images (right panels). (B) Mean ratios of nuclear/cytosolic phospho-CaMKIV labelling in control cells or cells subjected to the different treatments. The results are expressed as the mean ± SE of the number of cells (n) indicated in the figure. (C) Knockdown of CaMKIV causes an increase in the mRNA abundance for the four AMPAR subunits. The values are expressed as the mean ± SE of six determinations obtained from two different cellular preparations (*$p<0.001$, t-test).

a medium containing lower K^+ concentrations for 24 h. A three- to ten-fold increase in the expression of the four mRNAs was observed when the concentration of extracellular K^+ was reduced. The expression of each of the subunits was inversely related to the $[K^+]$ (stronger expression at lower $[K^+]$), except for GluR1, which reached a maximal expression at 15 mM K^+, decreasing thereafter as the $[K^+]$ diminished to 10 or 5 mM even though its content remained higher than in control cells (Fig. 3A). The specificity of the effect was confirmed by the fact that other mRNA levels tested as that encode for the α2 subunit of soluble guanylyl cyclase did not change (results not shown). The expression of these mRNAs was also analyzed in freshly isolated cells and cells maintained 14 days in culture (Supplementary material Fig. S2).

The integrity of the culture was analyzed by measuring the release of LDH, which remained similar in all the conditions tested (control: 7.97 ± 1.72%; 15 mM K^+: 7.15 ± 1.18%; 10 mM K^+: 9.80 ± 1.37%; 5 mM K^+: 9.82 ± 1.30%). The presence of 25 mM K^+ in the culture medium produces a tonic depolarization that enhances calcium entry via VSCCs, which activates different signalling pathways. To determine whether the reduced calcium entry into cells exposed to lower $[K^+]$ mediated the upregulation of AMPAR mRNA expression, the effects of antagonists to the different VSCCs expressed by these cells was assessed. No change in the four mRNAs was detected after 24 h in the presence of ω-Conotoxin GVIA (2 μM) to block N-type calcium channels, or SNX (400 nM) to block the R-type channels (Fig. 3B). However, in the presence of nifedipine (5 μM), which block L-type

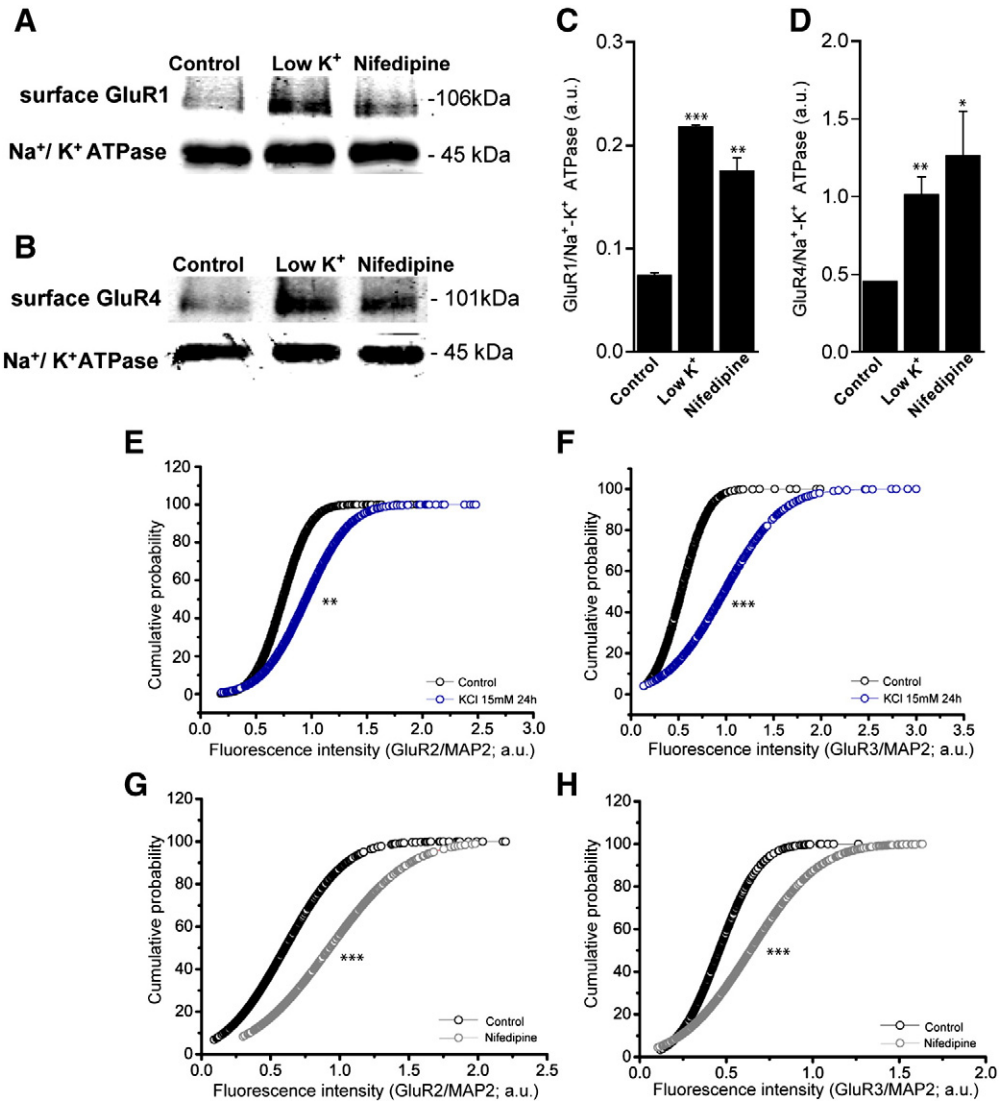

Fig. 7. The AMPAR subunits at the plasma membrane augments when extracellular K^+ is reduced or L-type VDCCs are blocked. (A) Representative Western blot to detect GluR1 in a plasma membrane enriched preparation from control cells, or cells maintained for 24 h in 15 mM K^+ or in the presence of 5 μM nifedipine. Detection of the β subunit of Na^+/K^+ ATPase served as a loading control. (B) Quantification of GluR1 normalized to the Na^+/K^+ ATPase content in control cells and in cells incubated in 15 mM K^+ or in the presence of 5 μM nifedipine. Data represent the mean ± SE from $n = 5$ experiments performed with different cell cultures. (C) Representative Western blot to detect GluR4 in a plasma membrane enriched preparation obtained from control cells and in cells maintained for 24 h in 15 mM K^+ or in the presence of 5 μM nifedipine. The β subunit of Na^+/K^+ ATPase served as a loading control. (D) Quantification of the amount of GluR4 normalized to the Na^+/K^+ ATPase content in control cells, and in cells incubated in 15 mM K^+ or in the presence of 5 μM nifedipine. The data are represented as the mean ± SE from $n = 4$ experiments performed with different cell cultures. Cumulative probability plots of mean GluR2/MAP-2 fluorescence intensity in non-permeabilized control cells versus cells incubated in 15 mM K^+ (E) or 5 μM nifedipine (F) (**$p < 0.01$, Mann–Whitney test and Kolmogorov–Smirnov test). Mean GluR2 intensity: 10.03 ± 0.53, 19.56 ± 2.91 and 20.28 ± 3.21 a.u. for control (970 ROIs), lower K^+ (931 ROIs), and 5 μM nifedipine, respectively (753 ROIs). Cumulative probability plots of mean GluR3/MAP-2 fluorescence intensity in non-permeabilized cells control cells versus cells incubated in 15 mM K^+ (G) or 5 μM nifedipine (H: ***$p < 0.001$, Mann–Whitney test and Kolmogorov–Smirnov test). Mean GluR3 fluorescence intensity: 20.32 ± 1.75, 36.86 ± 1.83 and 35.76 ± 2.23 a.u. for control (563 ROIs), low K^+ (650 ROIs), and 5 μM nifedipine (732 ROIs), respectively.

calcium channels, the abundance of each of the four mRNAs increased to a similar extent (GluR1: 2.53 ± 0.09-fold; GluR2: 2.90 ± 0.11-fold; GluR3: 2.75 ± 0.28-fold, and GluR4: 2.47 ± 0.08-fold). Higher concentrations of nifedipine did not produce larger increases in the mRNAs, suggesting that calcium entry through L-type channels was completely inhibited by 5 μM nifedipine and that the reduction in calcium entry due to the decrease in extracellular [K^+] was at least in part responsible for the effects observed. Moreover, when P/Q-type calcium channels were blocked with ω-Agatoxin IVA (500 nM), only the mRNA encoding GluR3 augmented, albeit to a lesser extent than when the L-type channels were blocked (control: 1.07 ± 0.02 and ω-Agatoxin IVA: 1.63 ± 0.03, $n = 9$; $p < 0.001$, t-test).

The increase in mRNAs levels observed when the extracellular [K^+] was reduced lead to an increase in the corresponding proteins as determined immunocytochemically. To evaluate the amount of these proteins in dendrites, double labelling with the corresponding antibody against each AMPAR subunit and anti-MAP-2 was used to normalize the fluorescence. Whereas the intensity due to MAP-2 labelling (Fig. 4A, B, and C) was equivalent in the controls and in cells switched to lower [K^+], the fluorescence intensity of GluR1 labelling increased by 37% in cells

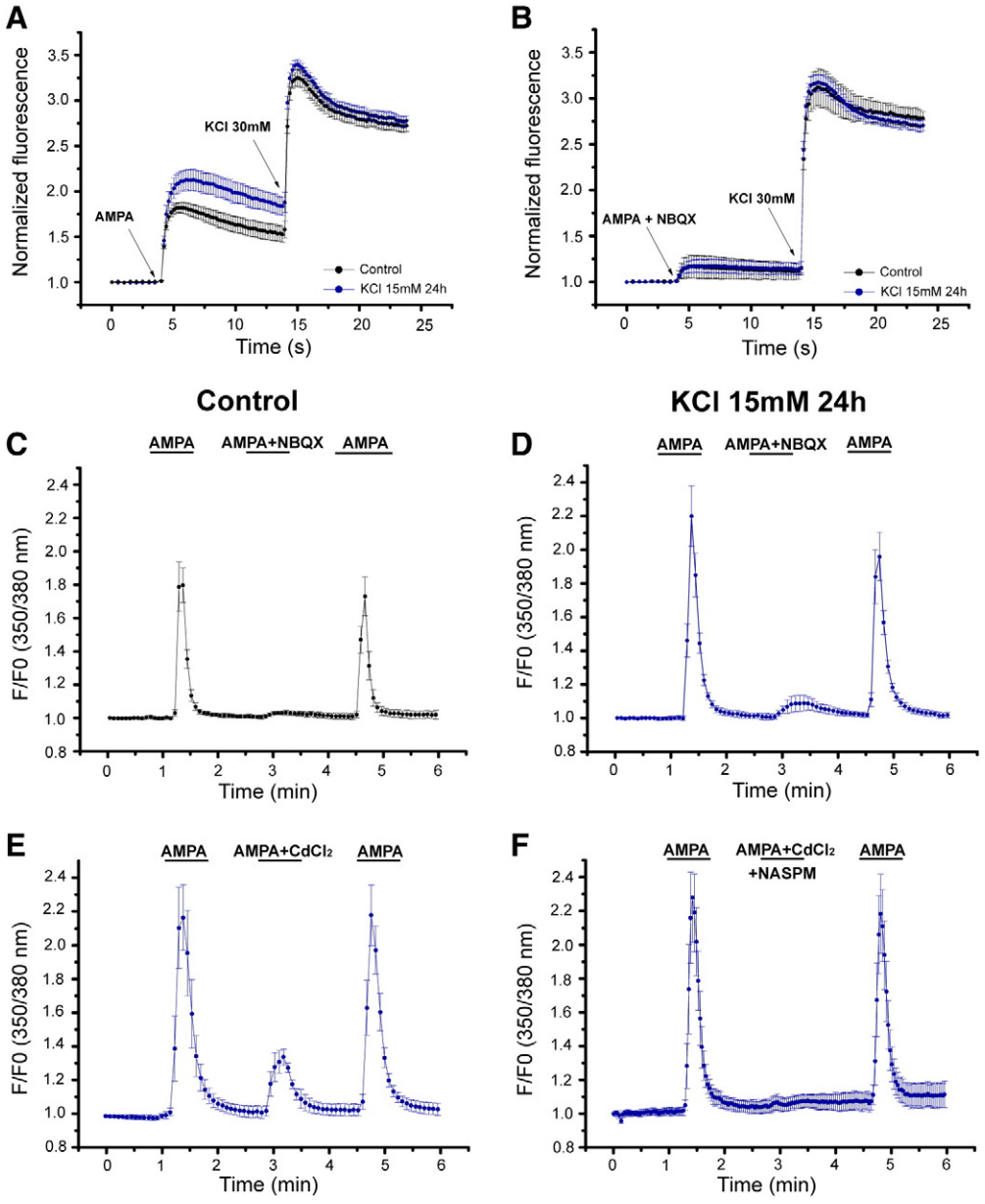

Fig. 8. AMPA stimulation triggers larger increases in calcium in cells incubated in 15 mM K^+. (A) Responses of cell populations cultured in 96-well microplates in control conditions (black traces) or switched to a lower K^+ containing medium (blue traces) stimulated with 50 μM AMPA + 10 μM cyclothiazide. (B) Cell populations cultured in 96-well microplates in control conditions (black traces) or maintained for the last 24 h in a medium containing a lower K^+ (blue traces) preincubated with 10 μM NBQX and then stimulated with 50 μM AMPA + 10 μM cyclothiazide. (C) Single-cell responses to 50 μM AMPA + 10 μM cyclothiazide stimulation (first and third peaks) or in the presence of 10 μM NBQX (second peak). The results represent the mean response of 35 cells cultured in control conditions. (D) Single-cell responses to 50 μM AMPA + 10 μM cyclothiazide stimulation (first and third peaks) or in the presence of 10 μM NBQX (second peak). The results represent the mean response of 37 cells cultured in 15 mM K^+ medium for the last 24 h. (E) Single-cell responses to 50 μM AMPA + 10 μM cyclothiazide stimulation (first and third peaks) or in the presence of 25 μM Cd^{2+} (second peak). The results represent the mean response of 51 cells cultured in 15 mM K^+ medium during the last 24 h. (F) Single-cell responses to 50 μM AMPA + 10 μM cyclothiazide stimulation (first and third peaks) or in the presence of 25 μM Cd^{2+} plus 10 μM 1-naphthyl acetyl spermine (NASPM) (second peak). The results represent the mean response of 52 cells cultured in 15 mM K^+ medium during the last 24 h.

incubated in 15 mM K^+ for 24 h (Fig. 4A, B, and D: the mean ratio of GluR1 fluorescence intensity/MAP-2 fluorescence intensity was 1.01 ± 0.01 for the controls and 1.39 ± 0.01 in low [K^+]; $p<0.001$, Mann–Whitney test and Kolmogorov–Smirnov test). Similar results were observed when the levels of GluR4 were analyzed where the mean fluorescence intensity for GluR4 increased by 43% in cells maintained in low [K^+] for 24 h (Fig. 4E–H: ratio GluR4 fluorescence/MAP-2 fluorescence, 1.05 ± 0.01 and 1.49 ± 0.02 for control and low [K^+]; $p<0.001$, Mann–Whitney test and Kolmogorov–Smirnov test). Similar values were observed when the analysis was performed on the somas (Supplementary material, Fig. S3).

In permeabilized cells labelled with anti-GluR2 and anti-MAP-2, there was no change in either MAP-2 fluorescence intensity (Fig. 5A, B, and C) or GluR2 intensity in dendrites (Fig. 5A, B, and D), whereby the ratio of GluR2 fluorescence/MAP-2 fluorescence was 0.60 ± 0.01 ($n=595$) in control conditions and 0.62 ± 0.01 ($n=490$) in low [K^+] ($p>0.05$, Mann–Whitney test and Kolmogorov–Smirnov test). Similar results were observed when cells were labelled with anti-MAP-2 (Fig. 5E, F, and G) and anti-GluR3 (Fig. 5E, F, and H). It is noteworthy that when the analysis was performed on the cell bodies, a 29% increase in GluR2/MAP-2 and a 33% increase in GluR3/MAP-2 fluorescence were observed in cells maintained in low K^+ medium, consistent with an increase in the abundance of these proteins that paralleled the increase in mRNAs (Supplementary material, Fig. S3).

3.2. Nuclear localization of phospho-CaMKIV in cells grown in high potassium may account for the inhibition of AMPAR subunit expression

Calcium/calmodulin-dependent protein kinases (CaMKs) are important mediators of many effects dependent on calcium, including the synaptic accumulation of AMPAR [32,33]. We tested whether there was a change in the abundance of active pCaMKs in the nucleus when the extracellular [K^+] was reduced or L-type calcium channels were blocked. Indeed, there was a clear reduction in the immunofluorescence of pCaMKIV in cells when the calcium influx was reduced (Fig. 6A). The nuclear/cytosolic ratio of immunostaining measured with an anti-phospho-CaMKIV antibody decreased significantly in both low [K^+] or in the presence of nifedipine (Fig. 6B). Moreover, transfection with specific siRNAs that caused the silencing of CaMKIV in 37 out of 57 cells (65%) increased AMPAR subunit mRNA expression (Fig. 6C).

3.3. Persistent reduction of neuronal activity enhanced the surface insertion of functional AMPARs

Since the antibodies used to detect GluR1 and GluR4 were raised against the C-terminal domain of these proteins, which resides at the cytosolic side of the plasma membrane, immunocytochemical studies were performed on permeabilized cells, which makes it impossible to distinguish receptors in the plasma membrane from those at intracellular structures. To evaluate whether these proteins (GluR1 and GluR4) augmented at the plasma membrane of cells when they were switched to lower [K^+], plasma membrane-enriched fractions were analyzed in Western blots. Switching cells to medium containing lower [K^+] produced an increase in both GluR1 (2.33 ± 0.12-fold) and GluR4 (2.27 ± 0.02-fold (Fig. 7; $p<0.05$, t-test) in the plasma membrane fraction, while the ratio of GluR4/GluR1 was not affected. Likewise, a similar increase in the presence of GluR1 by (2.90 ± 0.31) and GluR4 by 2.76 ± 0.24 (Fig. 7B and D; $p<0.05$, t-test) in the plasma membrane fraction was observed when L-type calcium channels were blocked.

The antibodies used to detect GluR2 and GluR3 were raised against the extracellular amino-terminal of these proteins, and hence, the presence of these proteins at the plasma membrane could be evaluated directly by immunolabelling under non-permeabilized conditions. MAP-2 immunofluorescence was not affected when cells were maintained for 24 h in lower [K^+] or in the presence of 5 μM nifedipine (data not shown), whereas GluR2 immunofluorescence augmented in these cells (Fig. 7E and G). This effect was reflected by the increase in the GluR2/MAP-2 fluorescence ratio from 0.74 ± 0.01 ($n=1099$) in control conditions to 0.95 ± 0.01 ($n=1052$) in low [K^+] medium ($p<0.001$, Mann–Whitney test and Kolmogorov–Smirnov test) or 0.89 ± 0.02 in the presence of nifedipine ($p<0.001$, Mann–Whitney test and Kolmogorov–Smirnov test). Similar results were observed for GluR3, with an increase in the GluR3/MAP-2 fluorescence ratio from 0.52 ± 0.01 to 0.97 ± 0.02 in low [K^+] and 0.93 ± 0.03 in the presence of nifedipine (Fig. 7F and H, $p<0.001$, Mann–Whitney test and Kolmogorov–Smirnov test). Conversely, the amount of the β subunit of the Na^+,K^+-ATPase, although not significantly, slightly decreased in cells subjected to the same treatment (Supplementary material, Fig. S4) when the fluorescence ratio ATPase/MAP-2 in non-permeabilized cells was analyzed.

The increase in intracellular calcium was used as a functional test of AMPA receptor activation to analyze whether the response to AMPA differed in cells maintained in a lower [K^+] medium for 24 h. AMPA triggered an increase in intracellular calcium when applied in combination with cyclothiazide, a response that augmented by 50% in cells maintained for 24 h in a lower [K^+] medium (Fig. 8). When performed in the cell population, the response to AMPA was normalized to that produced by 30 mM K^+ in order to correct for any variation in cell number, whereby the ratios obtained were 0.79 ± 0.05 ($n=8$) in control conditions and 1.03 ± 0.05 ($n=7$) in cells maintained in a low [K^+] (Fig. 8A, $p<0.05$ t-test). When individual cells were analyzed by calcium imaging, similar effects were observed whereby the fluorescence ratio F/F_0 increased from 0.66 ± 0.05 in control conditions ($n=35$ cells) to 1.17 ± 0.02 ($n=37$ cells) in low [K^+] (Fig. 8C and D, $p<0.001$, t-test). The specificity of the response was confirmed by its abolition in the presence of the AMPAR antagonist NBQX (Fig. 8B–D).

To determine the contribution of calcium entry through VSCCs, these responses were studied in the presence of Cd^{2+} to non-specifically block VSCCs. The presence of Cd^{2+} completely abolished the response to 50 mM KCl stimulation (Fig. S5) but not that in response to AMPA (Fig. 8E). To avoid the possible contribution of calcium entry through NMDA receptors, the antagonist MK-801 was also present in some experiments (Table 2). The response to AMPA stimulation was partially inhibited by Cd^{2+} and MK-801, and it was inhibited to a similar extent by each compound alone or when added together in both control and low [K^+] conditions. The extent of inhibition achieved with Cd^{2+} alone, or in conjunction with MK-801, was slightly but consistently higher in calcium imaging experiments than in microplate experiments. These compounds partially occluded one another when added together, and they did not totally inhibit the AMPA-induced increase in calcium, suggesting that calcium still entered through calcium-permeable AMPA

Table 2
Blockage of the increase in intracellular calcium elicited by AMPA.

Treatment	Control (25 mM K^+)		15 mM K^+	
	Multiwell reader	Calcium imaging	Multiwell reader	Calcium imaging
NBQX (10 μM)	100% ($n=6$)	$94.9 \pm 2.2\%$ ($n=4$)	100% ($n=5$)	$97.0 \pm 2.1\%$ ($n=4$)
$CdCl_2$ (25 μM)	$57.9 \pm 3.0\%$ ($n=7$)	$68.2 \pm 2.6\%$ ($n=3$)	$58.3 \pm 2.9\%$ ($n=7$)	$72.7 \pm 1.5\%$ ($n=6$)
MK-801 (20 μM)	$26.9 \pm 0.9\%$ ($n=5$)	$24.5 \pm 1.2\%$ ($n=4$)	$21.0 \pm 3.0\%$ ($n=5$)	$26.0 \pm 1.0\%$ ($n=4$)
MK-801 + $CdCl_2$	$63.5 \pm 3.0\%$ ($n=6$)	$77.0 \pm 2.3\%$ ($n=4$)	$58.9 \pm 4.5\%$ ($n=5$)	$80.5 \pm 1.2\%$ ($n=4$)

Data represent the mean ± SE of n experiments performed in quadruplicate in the case of the Multiwell reader, and 8-10 cells analyzed in each calcium imaging experiment.

receptors. Since the response to AMPA in cells cultured in low [K^+] was higher than that in control cells and the proportion of the response inhibited by Cd^{2+} and MK-801 was similar in both situations, the remaining response resistant to Cd^{2+} and MK-801 inhibition was also greater in cells cultured in low [K^+], consistent with an increase in the Ca^{2+}-permeable AMPA receptors at the cell surface. This supposition was confirmed by the use of 1-naphthyl acetyl spermine (NASPM), a synthetic analogue of Joro spider toxin (JSTX) that specifically blocks the Ca^{2+}-permeable AMPA receptors because the calcium increase elicited by AMPA was completely abolished by $CdCl_2$ plus NASPM (Fig. 8F).

3.4. Persistent reduction of neuronal activity does not affect GluR2 mRNA edition

The impermeability to calcium of AMPA receptors is controlled by the presence of the (Q/R) edited form of the GluR2 subunit. We determined the extent of GluR2 mRNA editing in the two experimental conditions, and we found that GluR2 mRNA was fully edited in both conditions. Edition of GluR2 produces a change of A to G that introduces a restriction site for *Aci*I and eliminates a *Bbv*I restriction site. *AciI* digested all the amplified fragments containing the (Q/R) edition sequence when RT-PCR was performed on RNA extracted from 7 DIV cells cultured in control conditions or when switched to low [K^+] for the last 24 h (Fig. 9A). By contrast, *Bbv*I was unable to digest any of the PCR products (Fig. 9B), even though it completely digested the pBR322 plasmid used as a positive control (Fig. 9C).

4. Discussion

It has previously been shown that rat CGCs in culture need elevated concentrations of K^+ to survive, mainly because membrane depolarization mimics the in vivo effect of the first innervation of granule cells by glutamatergic mossy fibers [16,34]. In this work, we have studied the expression of the four subunits of AMPAR in CGCs, showing that a reduction in the K^+ concentration in the culture medium for 24 h affects AMPA receptor behavior by increasing (i) AMPAR subunit mRNA and protein expression, (ii) their presence at the plasma membrane, and (iii) the AMPA-elicited rise in calcium. Cells isolated directly from 7-day-old rat pups expressed the four mRNAs that encode AMPAR subunits, the most abundant being those encoding GluR1 and GluR4, as indicated previously [9]. The abundance of the four mRNAs decreases in cells cultured in standard conditions (25 mM K^+), although GluR1 and GluR4 mRNAs remain the most abundant at 7 or 14 days, and they are less strongly diminished than GluR2 and GluR3. This downregulation was presumed to be mainly due to the presence of high [K^+] in the culture medium since the reduction in the [K^+] was inversely correlated to a large increase in the expression of the mRNAs for the distinct receptor subunits. Indeed, it has been previously demonstrated that the expression of different AMPAR subunits in culture is regulated by epigenetic factors such as K^+-induced membrane depolarization [8,35]. However, developmental downregulation cannot be disregarded because GluR2 and GluR3 immunoreactivity in sections of the P14 rat cerebellum was intense in the EGL yet almost absent or very weak in the IGL.

We also show that blocking L-type Ca^{2+} channels produces an increase in the expression of the four mRNAs, in agreement with the upregulation of GluR1 and its insertion into the membrane of cells in the neuronal cortex following persistent blockage of L-type Ca^{2+} channels [36]. Indeed, a rise in intracellular calcium mediates a decrease in AMPAR mRNA expression in hippocampal neurons [37]. However, specific mechanisms might control the expression of each subunit, as reflected by the selective increase in GluR3 mRNA when P/Q-type channels are blocked, indicating that not only the amount of calcium that enters the cell is important but also the way by which it enters.

A drop in somatic calcium influx is sensed by a drop in activated nuclear CaMKIV, which then triggers an increase in AMPAR accumulation at the membrane of neocortical neurons [33]. Indeed, we found that a reduction in extracellular K^+ or the blockage of L-type calcium channels causes a decrease in the nuclear localization of the activated form of CaMKIV (p-CaMKIV) and that the silencing of this protein with specific siRNAs is correlated with a significant increase in AMPAR mRNA expression. Thus, CaMKIV directly or indirectly regulates AMPAR subunit expression in cerebellar granule cells, and probably their insertion into the membrane, as described in neocortical neurons [33].

All four protein subunits were detected by immunocytochemistry in 7 DIV cells, and the reduction in K^+ also produced an upregulation in the expression of these proteins. Moreover, we also observed an increase of the four subunits in the membrane, indicating that the adaptation to the new culture conditions also favors their insertion into membranes. In agreement with the increase in the number of receptors at the plasma membrane, the AMPA-elicited increase in calcium is enhanced in cells incubated in low K^+ containing medium. Thus, our results are compatible with the existence of both calcium-permeable and calcium-impermeable receptors. The existence of calcium-permeable receptors is supported by the Cd^{2+} and MK-801-resistant component that permitted calcium entry through permeable AMPAR since the AMPA-elicited increase in calcium was not completely inhibited by blocking VSCCs and NMDAR but it was totally abolished by blocking VSCCs and inhibiting the Ca^{2+}-permeable AMPA receptors. The existence of calcium-impermeable receptors is supported by the detection of GluR2 at plasma membrane and by the fact that the mRNA encoding GluR2 is completely edited at the Q/R site, indicating that the receptors containing the GluR2 subunit should be calcium-impermeable [7].

In summary, our results demonstrate that cerebellar granule cells express the four subunits of AMPA receptors, both in vitro and in vivo. Our observations also suggest that K^+-induced depolarization can regulate the abundance of AMPAR subunits and their insertion into the plasma membrane through a mechanism that involves calcium entry through L-type channels and the activation of CaMKIV. The

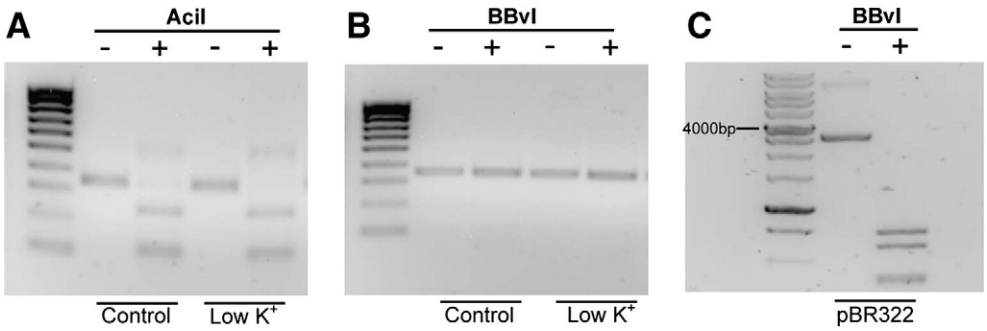

Fig. 9. GluR2 mRNA edition. Agarose gel showing PCR products that contain the Q/R site of GluR2 mRNA obtained from cells cultured in control or low K^+ concentration conditions, with (+) or without (−) AciI digestion (A), or with (+) or without (−) BbvI digestion (B). (C) Positive control showing BbvI activity using the pBR322 plasmid as substrate.

decreases in calcium entry caused by a reduction in depolarizing conditions leads to an increase in the number of AMPAR at the plasma membrane the activation of which could compensate this reduction in calcium.

Supplementary materials related to this article can be found online at doi:10.1016/j.bbamcr.2010.10.016.

Acknowledgments

This study was financed by grants from the Ministerio de Ciencia e Innovación (BFU2006-01012/BFI; BFU2009-07092 (subprograma BFI), the Ministerio de Sanidad y Consumo (RD06/0026/0001), the Comunidad de Madrid (S-BIO-0170/2006), and the UCM-CAM (CCG07-UCM/SAL-2150). S. Incontro was supported by a fellowship from the Spanish Ministry of Science and Innovation (MICINN), and J. Ramírez-Franco was supported by the Comunidad de Madrid. We thank Dr. Carmen Rúa and Javier Díaz for their help in immunohistochemistry experiments, and Dr. M. Sefton for the editorial assistance.

References

[1] N.A. Sans, M.E. Montcouquiol, J. Raymond, Postnatal developmental changes in AMPA and NMDA receptors in the rat vestibular nuclei, Brain Res. Dev. Brain Res. 123 (2000) 41–52.
[2] K.L. Moulder, R.J. Cormier, A.A. Shute, C.F. Zorumski, S. Mennerick, Homeostatic effects of depolarization on Ca^{2+} influx, synaptic signaling, and survival, J. Neurosci. 23 (2003) 1825–1831.
[3] N.Z. Gerges, D.S. Backos, C.N. Rupasinghe, M.R. Spaller, J.A. Esteban, Dual role of the exocyst in AMPA receptor targeting and insertion into the postsynaptic membrane, EMBO J. 25 (2006) 1623–1634.
[4] I.H. Greger, J.A. Esteban, AMPA receptor biogenesis and trafficking, Curr. Opin. Neurobiol. 17 (2007) 289–297.
[5] K. Borges, R. Dingledine, AMPA receptors: molecular and functional diversity, Prog. Brain Res. 116 (1998) 153–170.
[6] R.J. Wenthold, K.W. Roche, The organization and regulation of non-NMDA receptors in neurons, Prog. Brain Res. 116 (1998) 133–152.
[7] P.H. Seeburg, M. Higuchi, R. Sprengel, RNA editing of brain glutamate receptor channels: mechanism and physiology, Brain Res. Brain Res. Rev. 26 (1998) 217–229.
[8] D.F. Condorelli, P. Dell'Albani, E. Aronica, A.A. Genazzani, G. Casabona, M. Corsaro, R. Balázs, F. Nicoletti, Growth conditions differentially regulate the expression of alpha-amino-3-hydroxy-5-methylisoxazole-4-propionate (AMPA) receptor subunits in cultured neurons, J. Neurochem. 61 (1993) 2133–2139.
[9] H.S. Mogensen, O.S. Jørgensen, AMPA receptor subunit mRNAs and intracellular $[Ca^{2+}]$ incultured mouse and rat cerebellar granule cells, Int. J. Dev. Neurosci. 18 (2000) 61–68.
[10] N.S. Cheung, F.Y. Carroll, J.A. Larm, P.M. Beart, S.F. Giardina, Kainate-induced apoptosis correlates with c-Jun activation in cultured cerebellar granule cells, J. Neurosci. Res. 52 (1998) 69–82.
[11] R.C. Carroll, E.C. Beattie, H. Xia, C. Luscher, Y. Altschuler, R.A. Nicoll, R.C. Malenka, M. von Zastrow, Dynamin-dependent endocytosis of glutamate ionotropic receptors, Proc. Natl Acad. Sci. USA 96 (1999) 14112–14117.
[12] B.K. Ha, S. Vicini, R.C. Rogers, J.C. Bresnahan, R.W. Burry, M.S. Beattie, Kainate-induced excitotoxicity is dependent upon extracellular potassium concentrations that regulate the activity of AMPA/KA type glutamate receptors, J. Neurochem. 83 (2002) 934–945.
[13] G. Garthwaite, J. Garthwaite, Differential sensitivity of rat cerebellar cells in vitro to the neurotoxic effects of excitatory amino acid analogues, Neurosci. Lett. 48 (1984) 361–367.
[14] G. Garthwaite, J. Garthwaite, Amino acid neurotoxicity: intracellular sites of calcium accumulation associated with the onset of irreversible damage to rat cerebellar neurones in vitro, Neurosci. Lett. 71 (1986) 53–58.
[15] I. Lauritzen, M. Zanzouri, E. Honoré, F. Duprat, M.U. Ehrengruber, M. Lazdunski, Membrane depolarization regulates AMPA receptor subunit expression in cerebellar granule cells in culture, J. Biol. Chem. 278 (2003) 32068–32076.
[16] V. Gallo, A. Kingsbury, R. Balázs, O.S. Jorgensen, The role of depolarization in the survival and differentiation of cerebellar granule cells in culture, J. Neurosci. 7 (1987) 203–2213.
[17] N. Hack, H. Hidaka, M.J. Wakefield, R. Balázs, Promotion of granule cell survival by high K^+ or excitatory amino acid treatment and Ca^{2+}/calmodulin-dependent protein kinase activity, Neuroscience 57 (1993) 9–20.
[18] A.E. West, E.C. Griffith, M.E. Greenberg, Regulation of transcription factors by neuronal activity, Nat. Rev. Neurosci. 3 (2002) 921–931.
[19] K. Suzuki, M. Sato, Y. Morishima, S. Nakanishi, Neuronal depolarization controls brain-derived neurotrophic factor-induced upregulation of NR2C NMDA receptor via calcineurin signalling, J. Neurosci. 25 (2005) 9535–9543.
[20] M. Okazawa, H. Abe, M. Katsukawa, K. Iijima, T. Kiwada, S. Nakanishi Role, of calcineurin signaling in membrane potential-regulated maturation of cerebellar granule cells, J. Neurosci. 29 (2009) 2938–2947.
[21] M.L. Vallano, B. Lambolez, E. Audinat, J. Rossier, Neuronal activity differentially regulates NMDA receptor subunit expression in cerebellar granule cells, J. Neurosci. 16 (1996) 631–639.
[22] L.M. Gault, R.E. Siegel, Expression of the $GABA_A$ receptor δ subunit is selectively modulated by depolarization in cultured rat cerebellar granule neurons, J Neuroscience 17 (1997) 2391–2399.
[23] S. Jurado, J. Sánchez-Prieto, M. Torres, Differential expression of NO-sensitive guanylyl cyclase subunits during the development of rat cerebellar granule cells: Regulation via *N*-methyl-D-aspartate receptors, J. Cell Sci. 116 (2003) 3165–3175.
[24] M.E. López-Jiménez, D. Bartolomé-Martín, J. Sánchez-Prieto, M. Torres, Suppression of guanylyl cyclase (beta1 subunit) expression impairs neurite outgrowth and synapse maturation in cultured cerebellar granule cells, Cell Death Differ. 16 (2009) 1266–1278.
[25] M. Noursadeghi, J. Tsang, T. Haustein, R.F. Miller, B.M. Chain, D.R. Katz, Quantitative imaging assay for NF-kappaB nuclear translocation in primary human macrophages, J. Immunol. Methods. 329 (2008) 194–200.
[26] T.W. Ridler, S. Calvard, Picture thresholding using an iterative selection method, IEEE Trans. Syst. Man Cybern. 8 (1978) 630.
[27] S. Jurado, J. Sánchez-Prieto, M. Torres, Elements of the nitric oxide/cGMP pathway expressed in cerebellar granule cells: biochemical and functional characterisation, Neurochem. Int. 45 (2004) 833–843.
[28] R. Ferrero, M. Torres, Prolonged exposure of chromaffin cells to nitric oxide down-regulates the activity of soluble guanylyl cyclase and corresponding mRNA and protein levels, BMC Biochem. 3 (2002) 26.
[29] S. Jurado, F. Rodríguez-Pascual, J. Sánchez-Prieto, F.M. Reimunde, S. Lamas, M. Torres, NMDA induces post-transcriptional regulation of alpha2-guanylyl-cyclase-subunit expression in cerebellar granule cells, J. Cell Sci. 119 (2006) 1622–1631.
[30] C. Millán, R. Luján, R. Shigemoto, J. Sánchez-Prieto, Subtype-specific expression of group III metabotropic glutamate receptors and Ca^{2+} channels in single nerve terminals, J. Biol. Chem. 277 (2002) 47796–47803.
[31] X. Lin, R.F. Bulleit, Insulin-like growth factor I (IGF-I) is a critical trophic factor for developing cerebellar granule cells, Brain Res. Dev. Brain Res. 99 (1997) 234–242.
[32] T.C. Thiagarajan, M. Lindskog, R.W. Tsien, Adaptation to synaptic inactivity in hippocampal neurons, Neuron 47 (2005) 725–737.
[33] K. Ibata, Q. Sun, G.G. Turrigiano, Rapid synaptic scaling induced by changes in postsynaptic firing, Neuron 57 (2008) 819–826.
[34] R. Balazs, O.S. Jorgensen, N. Hack, *N*-methyl-D-aspartate promotes the survival of cerebellar granule cells in culture, Neuroscience 27 (1988) 437–451.
[35] N.J. Hack, A.A. Sluiter, R. Balfizs, AMPA receptors in cerebellar granule cells during development in culture, Dev. Brain Res. 87 (1995) 55–61.
[36] B. Gong, H. Wang, S. Gu, S.P. Heximer, M. Zhuo, Genetic evidence for the requirement of adenylyl cyclase 1 in synaptic scaling of forebrain cortical neurons, Eur. J. Neurosci. 26 (2007) 275–288.
[37] S.Y. Grooms, K.-M. Noh, R. Regis, G.J. Bassell, M.K. Bryan, R.C. Carroll, R.S. Zukin, Activity bidirectionally regulates AMPA receptor mRNA abundance in dendrites of hippocampal neurons, J. Neurosci. 26 (2006) 8339–8351.